

Photoacoustic Measurements of Thermal Conductivity of Crystalline RDX

Hackjin Kim*, Byung-Gook Kim†, Yong-Seok Lee†, and Joong-Gill Choi†

Department of Chemistry, Chungman National University, Taejon 305-764, Korea

†Department of Chemistry, Yonsei University, Seoul 120-749, Korea

Received August 31, 1995

Thermal conductivity acts as an important parameter in various dynamics of solids.¹ Thermal conduction in insulating atomic solids occurs mainly through lattice vibrations called phonons, however, molecular solids have different energy structure from atomic solids.² There exist localized molecular vibrations in addition to delocalized phonons and interactions of phonons and molecular vibrations make the dynamics of molecular solids complicated. Spatial propagation of chemical reactions in condensed phases may be understood as thermal conduction accompanied by chemical modifications of constituents in a broad sense.³ Most reaction energy is initially located in the vibrational modes of products and vibrational excitations transport into neighboring molecules via complex intra- and intermolecular processes.

A lot of theoretical studies have been carried out for thermal conduction in insulating atomic solids and a simple phonon gas model explains well temperature dependence of thermal conductivity.⁴ Thermal conductivity is expressed in terms of heat capacity, velocity of phonons, and mean free path of phonon scattering in the phonon gas model. Temperature dependence of the phonon scattering processes appears in thermal conductivity. Two different mechanisms are effective in the scattering of phonons - normal and umklapp process. The Debye temperature (θ_D) is an important parameter in the thermal conduction of crystalline phases because heat capacity and phonon population depend on θ_D .

Thermal conductivity is generally determined from rates of temperature change in a sample with temperature gradient.⁵ Photoacoustic spectroscopy (PAS) has been employed as a promising technique for the measurement of thermal conductivity.^{6,7} In PAS, variation of the ambient pressure around a sample is detected, which results from thermal expansion of a medium by heat released from the sample. Transformation of absorbed radiation energy into thermal energy is affected by optical and thermodynamic properties. PAS signals are also sensitive to experimental methods and sample conditions such as thickness. Extensive theoretical studies have been carried out for the analysis of various cases of PAS.^{6,8}

Experimental

Hexahydro-1,3,5-trinitro-1,3,5-s-triazine (RDX) is purified by recrystallization several times with spectrograde acetone and single crystals of a few mm order are grown by slow evaporation of saturated solution at room temperature. X-ray diffraction data of the grown crystals show good agreement

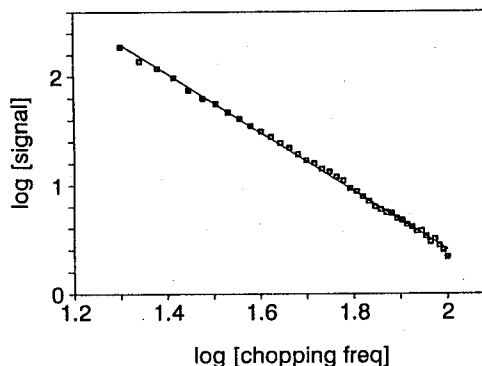


Figure 1. Chopping frequency dependence of the PAS signal for RDX at 130 K. The uv output at 340 nm from Ar ion laser is employed as a light source and the light intensity at the sample is about 10 mW/cm². The data are collected at intervals of 2 Hz from 20 to 100 Hz. The slope of the solid line is -1.35.

with the known cell parameters.⁹ RDX is an energetic material widely used as secondary explosives.¹⁰ Carbon black (CB, Aldrich) powder is used as a reference material.

A conventional PAS experimental setup using gas-microphone method is employed in this work. Details of the experimental setup for PAS are previously reported¹¹ and only brief description of the experimental setup is given. The PAS cell made of copper is cooled down with liquid nitrogen and nitrogen gas is used as a medium transmitting pressure variations to the microphone. High power Xe lamp (300 W) or Ar ion laser modulated by a mechanical chopper is used as a light source.

Results and Discussion

Photoacoustic characteristics are classified depending on sample thickness, absorption and thermal diffusion coefficients, and chopping frequency of incident light.⁶ Figure 1 shows the chopping frequency dependence of the PAS signals of the RDX crystal. The frequency dependence of the PAS signal, $\omega^{-1.35}$, indicates that the RDX crystals are thermally thick.⁶ Since the absorption coefficient of the crystalline RDX is about 200 cm⁻¹ at 340 nm¹² and the sample thickness is greater than 1 mm, the RDX crystals are optically opaque at the experimental conditions. The wavelength of the incident light is chosen in order to avoid photochemical reactions of RDX.

The PAS intensity of optically opaque and thermally thick samples like the RDX crystal, Q_{RDX} , is given by⁶

$$Q_{RDX} \propto (\mu/\kappa)_{RDX}/A_{gas} \quad (1)$$

where μ and κ are thermal diffusion length and thermal conductivity respectively and A is thermal diffusion coefficient. Thermal diffusion length, the inverse of the thermal diffusion coefficient, is defined as $[2\kappa/\rho C\omega]^{1/2}$ where ρ and C are density and heat capacity respectively and ω is the chopping frequency of the incident light. The subscripts of Eq. (1) denote the RDX sample and the ambient gas. The proportional constant related to the experimental conditions and optical properties of a sample is usually determined by calibration with the results of reference materials.

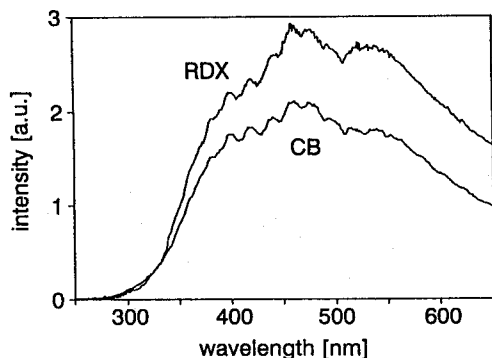


Figure 2. Photoacoustic spectra of carbon black (CB) and RDX at 130 K. The spectra consist with the power spectrum of the light source, Xe lamp. The chopping frequency of 18 Hz and the resolution of the spectra is 1 nm.

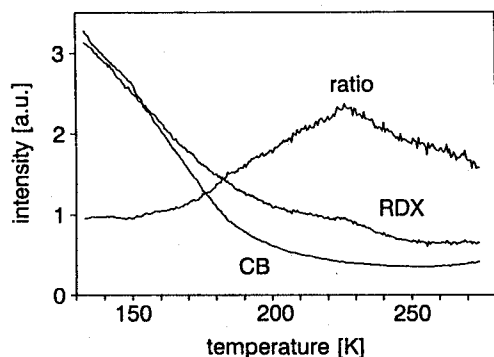


Figure 3. PAS signals of carbon black (CB), RDX and their ratio in the temperature range from 130 K to 270 K. The light of 320 nm from Xe lamp is used as the light source and the light intensity at the sample is about 100 mW/cm². The data are collected by every 0.5 K and the chopping frequency is 75 Hz.

The PAS intensity of optically opaque and thermally thin samples like CB powder, Q_{CB} , is given by⁶

$$Q_{CB} \propto (\mu/\kappa)_{back}/A_{gas} \quad (2)$$

The same notations are used in Eq. (2) as Eq. (1). The subscript of back in Eq. (2) denotes the backing material for the sample. The PAS spectra of the RDX crystals and CB powder shown in Figure 2, which are consistent with the power spectrum of the light source, Xe lamp, support that Eqs. (1) and (2) are valid for the PAS characteristics of the samples.

Figure 3 shows the signal intensities of the CB and RDX crystal and their ratios. From Eqs. (1) and (2), the expression for thermal conductivity of the RDX sample is given by

$$[\kappa]_{RDX}/[Y_{RDX}/Y_{CB}]^2 = \{[\kappa\rho C]_{back}/[\rho C]_{RDX}\}/R^2 = K \quad (3)$$

where Y 's are the proportional constants for Eqs. (1) and (2), and R corresponds to the ratio of Q_{RDX}/Q_{CB} . Note that all parameters in Eq. (3) change with temperature. Since thermal expansion coefficients of organic crystals and metals are in the order of 10^{-4} or 10^{-5} ,^{13,14} density changes of the RDX crystals and backing material copper are negligible in

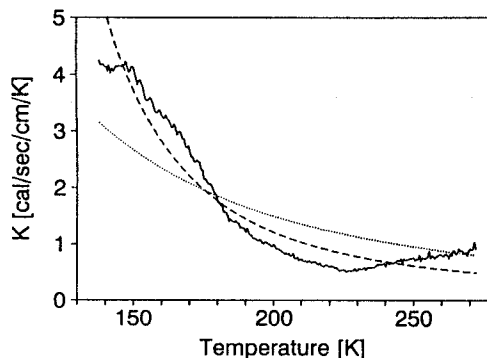


Figure 4. Plot of the K value of Eq. (3) (solid line). The best fitting curves of the exponential function ($\exp(T_0/T)$, dashed line) and the power law ($1/T^2$, dotted line) are plotted together. The fitting parameter for the exponential function, T_0 is 670 K.

the studied temperature range.

The quantity K of Eq. (3) calculated from the ratio of the signal intensities for CB and RDX crystal, the known thermal parameters for copper¹⁴ and heat capacity of the crystalline RDX¹⁵ is plotted in Figure 4 with some theoretical fitting curves. Thermal conductivity of solid RDX measured at room temperature is reported to be 6.98×10^{-4} cal/sec/cm/K¹⁶ and the same unit is used for the K values of Figure 4. Discrepancy of the K values and the reported thermal conductivity of the RDX crystal results from the proportional constants. Among many parameters involved in the proportional constant, only efficiencies of non-radiative decay are different for RDX and CB samples when the experimental conditions are identical. The K values greater than the reported thermal conductivity indicate that the RDX crystal has smaller efficiency of non-radiative decay than CB. Since the efficiency of non-radiative decay for CB is almost one,⁶ the efficiency of non-radiative decay of the RDX crystal is estimated to be in the range of 10^{-1} - 10^{-2} , which seems to be reasonable for organic molecular crystals.¹⁷ The calibration factor for the conversion of the K value into the thermal conductivity of the RDX crystal is 1×10^{-4} in the observed temperature range. The change of the thermal conductivity of the RDX crystal by a factor of four in the experimental temperature range is reasonable compared with other organic materials.¹⁸

According to the phonon gas model,³ normal and umklapp processes compete at higher temperatures than θ_D . Umklapp processes reveal temperature dependence of $\exp(T_0/T)$ where T_0 is a temperature of order θ_D . As the temperature range investigated in this work is higher than θ_D of the RDX crystal, about 60 K,¹⁵ temperature dependence of umklapp processes is reduced to $1/T$. Normal processes show temperature dependence of $1/T^n$ where n is between 1 and 2, which is related with the number of phonons involved in the scattering.^{19,20}

The best fitting parameter for umklapp processes shown in Figure 4 is 670 K, which is much larger than θ_D of the RDX crystal. The exponential function with θ_D of the RDX crystal is almost flat in the temperature range of 130 K to 270 K. The fitting parameter much greater than θ_D indicates that the exponential behavior is not valid in the experimental temperature range. The best fit of the power law for $n=2$ is shown in Figure 4.

Several things can be considered for discrepancies of the K values and theoretical fittings. Constant efficiencies of non-radiative decay are assumed in Eq. (3), however, the efficiency of non-radiative decay usually decreases at low temperature. If the reduced efficiency of non-radiative decay is used at low temperatures, the consistency of the K values and the power law would be improved. Participation of molecular vibrations in thermal conduction of molecular crystals^{2,3,20} is not considered in the simple phonon gas model. At very low temperature below θ_D , thermal conduction occurs mainly by phonons. When temperature rises to produce sufficient population of phonons, low lying vibrations are excited and complex dynamics of molecular vibrations activate. Among various vibrational relaxation processes responsible for the spatial energy transport, resonant intermolecular vibrational energy transfer is significant at low temperatures and interrupted with temperature rise.^{2b} Deviation from the power law may be interpreted as the results of direct resonant intermolecular vibrational energy transfer.

Acknowledgment. This work was supported by Basic Science Research Institute Program, Ministry of Education of Korea and by Korea Science and Engineering Foundation.

References

1. Kittel, C. *Introduction to Solid State Physics*; 5th Ed.; McGraw-Hill: New York, U.S.A., 1976.
2. (a) Kim, H.; Dlott, D. D. *J. Chem. Phys.* **1991**, *93*, 8203. (b) Kim, H.; Dlott, D. D.; Won, Y. *J. Chem. Phys.* **1995**, *102*, 5480.
3. (a) Dlott, D. D.; Fayer, M. D. *J. Chem. Phys.* **1990**, *92*, 3798. (b) Tokmakoff, A.; Fayer, M. D.; Dlott, D. D. *J. Phys. Chem.* **1993**, *97*, 1901.
4. Ashcroft, N. A.; Mermin, N. D. *Solid State Physics*; Holt: New York, U.S.A., 1976.
5. Hust, J. G. *Thermal Conductivity*; Plenum: New York, U.S.A., 1983.
6. Rosenzweig, A. *Photoacoustic and Photoacoustic Spectroscopy*; Wiley: New York, U.S.A., 1980.
7. (a) Madhusoodanam, K. N.; Thomas, M. R.; Philip, J. *J. Appl. Phys.* **1987**, *62*, 1162. (b) Ahlers, G.; Cannel, D. S.; Berge, L. I.; Sakurai, S. *Phys. Rev. E* **1994**, *49*, 545.
8. (a) Marinelli, M.; Zammit, U.; Scudieri, F.; Martellucci, S.; Quartieri, J.; Bloisi, F.; Vicari, L. *IL NUOVO CIMENTO* **1987**, *9*, 557. (b) Marinelli, M.; Zammit, U.; Scudieri, F.; Martellucci, S.; Bloisi, F.; Vicari, L. *IL NUOVO CIMENTO* **1987**, *9*, 855.
9. Choi, C. S.; Prince, E. *Acta Cryst.* **1972**, *B28*, 2857.
10. Bulusu, S. N. *Chemistry and Physics of Energetic Materials*; Kluwer: Dordrecht, Germany, 1990; Nato ASI Series C Vol. 309.
11. Bak, Y. H.; Chu, J. H.; Kang, B. K.; Kwag, J. H.; Kim, U.; Hwang, J. S.; Choi, J. G.; Kim, C. S. *J. Kor. Phys. Soc.* **1991**, *24*, 489.
12. Marinkas, P. L.; Mapes, J. E.; Downs, D. S.; Kemmey, P. J.; Forsyth, A. C. *Mol. Cryst. Liq. Cryst.* **1976**, *35*, 15.
13. Krishnan, R. S.; Srinivasan, R.; Devananyanan, S. *Thermal Expansion of Crystals*; Pergamon: Oxford, U.K. 1979.
14. Weast, R. C. *CRC Handbook of Chemistry and Physics*; 67th Ed.; CRC: Boca Raton, U.S.A., 1986.
15. Rey-Lafon, M.; Bonjour, E. *Mol. Cryst. Liq. Cryst.* **1973**,

24, 191.

16. Fedoroff, B.; Sheffield, O. E. *Encyclopedia of Explosives and Related Items*; Picatinny Arsenal: Dover, U.S.A., 1966; Vol. 3.
17. Marinkas, P. L. *J. Lumin.* **1977**, *15*, 57.
18. Yarbrough, D. W.; Kuan, C.-N. In *Thermal conductivity 17*; Hust, J. G., Ed.; Plenum: New York, U.S.A., 1983.
19. Herring, C. *Phys. Rev.* **1954**, *95*, 954.
20. Kim, H.; Dlott, D. D. *J. Chem. Phys.* **1990**, *93*, 1695.

Potentiometric Study of Co(II), Ni(II), Cu(II), and Zn(II) Complexes of Pyridyl- and Pyrrolyl-Containing Triethylenetetramine Ligands

Sun-Deuk Kim*, Jun-Kwang Kim, and Woo-Sik Jung†

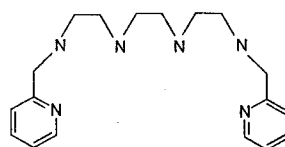
Department of Chemistry, Taegu University,
Kyongsan 713-714, Korea

†Department of Industrial Chemistry,
Yeungnam University,
Kyongsan 712-749, Korea

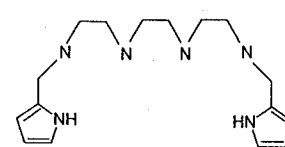
Received September 11, 1995

The role of transition metal ions in the redox functions of various enzymes in the living systems has been extensively studied by using synthetic model complexes.¹ Many of the complexes are those of Schiff bases which are synthesized from the condensation reaction between *ortho*-substituted aromatic aldehydes and various primary amines.² The Schiff base complexes which contain -CH=N bonds are usually insoluble or unstable in water. In contrast, the metal complexes of ligands which are obtained by hydrogenation of -CH=N bonds in Schiff bases are soluble and stable in water. The hydrogenation is unlikely to affect their coordination ability to form strong bonds with transition metal ions. The hydrogenated ligands are more flexible than the parent compounds and which thus can present their donor atoms to a metal atom from either a planar or a nonplanar arrangement.³

Martell *et al.* studied the interaction of pyridyl- and imidazolyl-containing ligands with a series of first-row transition metals and showed that the stability constants of the ligands are higher than those of the analogous aliphatic polyamines.⁴⁻⁷ This study deals two ligands, 1,12-bis(2-pyridyl)-2,5,8,11-tetraazadodecane (pytrien) and 1,12-bis(2-pyrrolyl)-2,5,8,11-tetraazadodecane (pyrrotrien) as their tetrahydrochloride salts. Proton association constants and stability constants of the ligands with Co(II), Ni(II), Cu(II), and Zn(II) ions are



pytrien



pyrrotrien